Coulomb Fission by Very Heavy Ions*

L. WILETS
University of Washington, Seattle, Washington

AND

E. GUTH
Oak Ridge National Laboratory, Oak Ridge, Tennessee

AND

J. S. TENN
University of Washington, Seattle, Washington

(Received 23 November 1966)

It is proposed that very heavy ions (including uranium) be utilized to induce fission through the Coulomb interaction only. Because the projectile moves slowly, the process is expected to be nearly adiabatic (no intrinsic excitation). Dynamical-model calculations have been performed at zero impact parameter to determine the threshold energy, cross section, and fragment angular distribution. Differential cross sections of hundreds of millibarns are calculated, and fission fragments are found to emerge preferentially at 90° in the pair frame. The calculations incorporate reasonable model data, but the equilibrium-to-saddle distance $\Delta\beta$ is unknown. In order for fission to occur below the Coulomb barrier, $\Delta\beta$ must be greater than 0.15 in the case of Cf, for example. Rotational and vibrational excitation is discussed for energies below the fission threshold. A primary objective of the experiments would be to determine $\Delta\beta$ (and the shape of the energy-deformation curve). This would provide a severe test of various nuclear-model theories.

I. INTRODUCTION

A. Deformation-Energy Surface

THE nuclear deformation-energy surface is a subject of considerable interest for many nuclear processes. It plays a vital role for collective states and for the fission reaction. A better experimental determination of the surface would not only improve our understanding of these processes, but also provide a severe test of the theoretical models which attempt to calculate the surface. Our current knowledge of the surface is incomplete in an important way. What is known experimentally can be summarized as follows.[1]

From the level structure and transition rates of the low-lying collective states, it has been possible to infer the equilibrium deformation (β_0), the associated force constants (C_β and C_γ), and the mass parameters (B_β and B_γ). The identifications of all of these quantities is, of course, model-dependent. β_0 is obtained from the $B(E2)$ for rotational transitions. The C and B for β- and γ-vibrational states is extracted from the energy levels $[\hbar\omega=\hbar(C/B)^{1/2}]$ and the transition rates $[B(E2)\propto(BC)^{-1/2}]$.

The height of the saddle ($\mathcal{E}_b$) is fairly well known from the "threshold" of the cross section. The uncertainty is due to important quantum barrier-penetration effects near threshold.

At the saddle point, there is available only a single parameter, which can be expressed in terms of an effective inverted oscillator frequency $\omega_b=(C_b/B_b)^{1/2}$. This is deduced either from spontaneous fission lifetimes or (in a model-dependent interpretation) from the behavior of the fission cross section at threshold. But since the mass parameter B_b is undetermined, the force constant cannot be deduced.

The situation is depicted in Fig. 1. What is completely unknown[2] is the location of the barrier $\beta_b\equiv\beta_0+\Delta\beta$. The purpose of this paper is to discuss an experiment which probes further details of the fission curve.

B. Fission Via Compound Nucleus

In contrast to spontaneous fission, all *induced* fission experiments to date are describable in terms of a compound nucleus intermediate state. Energy is deposited into a target nucleus by particles or an electromagnetic

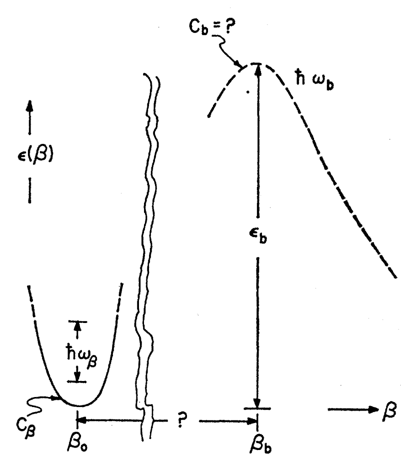

FIG. 1. Current status of experimental information on the nuclear energy-deformation surface. The quantity $\Delta\beta=\beta_b-\beta_0$ is completely unknown. So also is the barrier curvature C_b. The inverted barrier frequency ω_b has been deduced using model-dependent arguments. The quantities C_β, $\omega_\beta=[C_b/B(\beta_0)]^{1/2}$, and β_0 are fairly well determined.

* Supported in part by the U. S. Atomic Energy Commission.

[1] See, for example, E. K. Hyde, I. Perlman, and G. T. Seaborg, in *The Nuclear Properties of the Heavy Elements* (Prentice-Hall Publishing Company, Inc., Englewood Cliffs, New Jersey, 1964), Vol. I, Chap. 3; E. K. Hyde, *ibid.*, Vol. III, Chap. 3; J. S. Fraser and J. C. D. Milton, Ann. Rev. Nucl. Sci. **16**, 379 (1966); V. E. Viola, Jr. and B. D. Wilkins, Nucl. Phys. **82**, 65 (1966).

[2] For a model-dependent inference of β_0, however, see R. F. Reising, G. L. Bate, and J. R. Huizenga, Phys. Rev. **141**, 1161 (1966).

pulse. The heated nucleus may then blunder its way through the maze of intrinsic states, eventually passing over the fission barrier. The deformation-energy surface is only the envelope of the lowest states available.

C. Fission without Intrinsic Excitation

It has been proposed by two of the authors[3] that the Coulomb field of a heavy ion may be used to distort a fissile, even-even nucleus so that it is slowly carried over the barrier with little internal excitation. This allows a study of the deformation-energy surface directly. There are other advantages to studying this mode of fission.

(1) When projectile energies are restricted to values sufficiently below the Coulomb barrier, only electric forces are involved in inducing the process. This lends an important cleanness to the interpretation.

(2) For sufficiently slow encounters, the process is dominated by nuclear states and electrostatic considerations. Although the idealization cannot be achieved, (and thus dynamics must be considered), nevertheless the heavy projectiles deemphasize the role of dynamics.

D. Relationship to Projected Accelerators

A new generation of heavy-ion accelerators and modification of some existing machines make Coulomb fission experiments appear feasible in the next few years. Indeed, the expectation of several groups is to accelerate all ions (through uranium) over the Coulomb barriers of all targets. One expectation of such machines is the production of superheavy nuclei. This exceeds the requirements of Coulomb fission, since it is essential here to remain below the Coulomb barrier.

In order to demonstrate the feasibility of experiments and to exhibit the main features of the reaction, we present here some sample calculations. The present work employs a simplified model for the process which, we believe, is nevertheless physically reasonable. Since the results are model-sensitive, several adjustable parameters have been varied, especially the location of the barrier. Calculations involving more complete and detailed physical models are in progress.

It is our hope to stimulate experiments in the field so that future calculations can be performed with the object of fixing parameters by fitting data.

II. THE PHYSICAL MODEL

A. Definition of Deformation Parameter

A collective description of the fissioning nucleus is employed. The nuclear shape, in the present calculation, is described by a single parameter, which may be taken as the quadrupole moment:

$$Q=2\langle\rho(\mathbf{r})r^2P_2(\cos\theta)\rangle\,, \qquad (1)$$

where $\rho(\mathbf{r})$ is the number density of protons, so that Q has the dimensions of an area. Only axially symmetric shapes are considered, which is to say that the shape parameter γ is frozen at zero. The choice of Q as the parameter does not limit the allowable shapes to pure quadrupole deformations, but merely characterizes the deformation by its quadrupole moment.

For small deformations of a uniformly charged nucleus, Q is related to the Bohr-Mottelson deformation parameter β by

$$Q=(9/5\pi)^{1/2}ZR_0^2\beta\,, \qquad (2)$$

where Z is the proton number and R_0 is the mean nuclear radius. For separated, spherical, equal density fragments, the quadrupole moment can be expressed in terms of the separation distance s,

$$Q=2(Z_1Z_2/Z)s^2. \qquad (3)$$

For dimensional convenience, *we use Eq. (2) as a definition of β in terms of Q, and use β instead of Q* in the formulation of the problem. For example, at late stages of the fission act, the nucleus indeed separates, and β can still be used to describe the separated system by the relation

$$\beta=\left(\frac{20\pi}{9}\right)^{1/2}\frac{Z_1Z_2}{Z^2}\left(\frac{s}{R_0}\right)^2\equiv\left(\frac{s}{s_0}\right)^2. \qquad (4)$$

In the case of uranium, for typical charge separation, $s_0\simeq9.2$ F. We always assume the same neutron and proton ratios between the fragments $A_1/A_2=Z_1/Z_2$.

B. The Energy Expression

All dynamics are treated classically. The energy of the target plus the energy of interaction with the projectile is written

$$E=\tfrac{1}{2}B(\beta)\dot{\beta}^2+\tfrac{1}{2}\mathcal{I}(\beta)\dot{\theta}^2+\mathcal{E}(\beta)+(ze^2Q/2r^3)P_2(\cos\theta')\,, \qquad (5)$$

where $B(\beta)$ is the inertial parameter for β motion, $\mathcal{I}(\beta)$ is the rotational moment of inertia, $\mathcal{E}(\beta)$ is the deformation energy, and z is the charge of the projectile. The quantities r and θ' describe the distance and orientation of the projectile relative to the center and the symmetry axis of the target; θ is the orientation of the symmetry axis of the target relative to the laboratory.

The interaction has been restricted here to the quadrupole term, even though the deformation admits higher-order moments. We know very little about higher-order moments when the deformation is small, but we estimate these as follows. For separated fragments, the interaction with a point projectile is

$$\frac{Z}{r}\sum_\lambda\left[Z_1\left(\frac{Z_2}{Z}\right)^\lambda+(-)^\lambda Z_2\left(\frac{Z_1}{Z}\right)^\lambda\right]\left(\frac{s}{r}\right)^\lambda P_\lambda(\cos\theta')\,.$$

Since $|P_\lambda|\leqslant1$, we find that the first few terms are

[3] E. Guth and L. Wilets, Phys. Rev. Letters **16**, 30 (1966).

down, relative to the quadrupole term, by

$$\frac{\lambda=3}{\lambda=2}\sim\frac{s}{r}\left[\frac{Z_2^2-Z_1^2}{Z^2}\right]\sim\frac{1}{3}\frac{s}{r},$$

$$\frac{\lambda=4}{\lambda=2}\sim\left(\frac{s}{r}\right)^2\frac{Z_2^3+Z_1^3}{Z^3}\sim\frac{1}{3}\left(\frac{s}{r}\right)^2.$$

Although the interaction is not important by the time the spheres are separated, we use this expression and evaluate s from Eq. (4). Our calculations show that s/r never exceeds $\frac{1}{2}$, so that the contribution of the higher multipoles is down by nearly an order of magnitude at worst.

The relative motion $[r(t)$ and $\theta(t)]$ of the projectile and the target is calculated for point charges (monopole moment). This is a fairly good approximation, since the relative energy is hundreds of MeV, while the quadrupole interaction energy is of the order of 10 MeV. The projectile trajectories are restricted here to head-on collisions (hence $\theta'=\theta$) in order to facilitate the calculations, and because these are the most effective collisions. It is experimentally feasible to select such collisions.

III. SLOW COLLISIONS

A. Threshold Behavior

If the collision were to take place very slowly, the nuclear deformation would adjust itself at each instant of time so that the potential energy in Eq. (5) would be a minimum; that is, so that the restoring force $-\partial\mathcal{E}/\partial\beta$ would equal the distorting force $ze^2(dQ/d\beta)P_2/2r^3$. For this case, we can set P_2 equal to its maximum *negative* value, -0.5. This gives a condition for the "infinitely slow" collision threshold, E_{th}^∞, namely,

$$\max\left(\frac{\partial\mathcal{E}}{\partial\beta}\right)\equiv\mathcal{E}_\beta=\left(\frac{9}{80\pi}\right)^{1/2}\frac{zZe^2R_0^2}{r_c^3},\tag{6}$$

where r_c is the radius of closest approach. With the relationship $E_{\text{th}}^\infty=zZe^2/r_c$, we find

$$E_{\text{th}}^\infty=1.74[\mathcal{E}_\beta(zZe^2/R_0)^2]^{1/3}.\tag{7}$$

A rough measure of $\mathcal{E}_\beta$ is obtained from the cubic formula [see Eq. (13) below] for $\mathcal{E}(\beta)$, which leads to

$$\mathcal{E}_\beta\approx3\mathcal{E}_b/2\Delta\beta,\tag{8}$$

so that we see that

$$E_{\text{th}}^\infty\approx2.0\left[\frac{\mathcal{E}_b}{\Delta\beta}\left(\frac{zZe^2}{R_0}\right)^2\right]^{1/3}.\tag{9}$$

This estimate is, of course, for infinitely slow collisions. The actual threshold energy will be seen below to be somewhat higher. The functional dependence is generally useful, however.

A limit on the observability of Coulomb fission is that the closest approach be outside the range of nuclear forces. Let us consider uranium on uranium and set $r_c>2R_0$; then with $R_0=r_0A^{1/3}$, $r_0=1.2$ F, we require

$$\frac{\mathcal{E}_b}{\Delta\beta}<\frac{Z^2e^2}{64R_0}=25.6\text{ MeV}.\tag{10}$$

For $\mathcal{E}_b\sim5.8$ MeV (uranium), this implies that only if $\Delta\beta\gtrsim0.23$ will the reaction proceed below the Coulomb barrier. For $\mathcal{E}_b\sim3.8$ MeV (Cf), the limit is $\Delta\beta\gtrsim0.15$. Perhaps r_0 of 1.2 is too small to be inserted for r_c in the left-hand side of Eq. (9), but for slow collisions between highly charged particles, the electrostatic polarization acts to reduce the internuclear distance at which nuclear forces enter.

B. The Slowness Criterion

Even for collisions involving projectiles as heavy as uranium, the condition of being "infinitely slow" is not sufficiently well satisfied to warrant neglect of dynamics. We have two frequencies to compare during the collision. One is the characteristic collision frequency, which, for Coulombic orbits can be taken to be

$$\omega_c=\frac{v}{r_c}=\left(\frac{2zZe^2}{Mr_c^3}\right)^{1/2}.\tag{11}$$

The other is the vibrational frequency ω_β. The ratio

$$\xi=\omega_\beta/\omega_c$$

is called, in the parlance of Coulomb excitation,[4] the "adiabaticity parameter." We are, in fact, concerned here with two kinds of adiabaticity. One is with respect to intrinsic excitations, and the other is with respect to collective motion. Here ξ is the *collective* adiabaticity parameter. If ξ is large compared with unity, the collision is slow, and the considerations of the previous section (III A) obtain.

If we use Eq. (6) to *estimate* ξ at the "adiabatic" threshold, we find

$$\xi_0\equiv\left(\frac{3}{8}\frac{MR_0^2\omega_\beta^2}{(5\pi)^{1/2}\mathcal{E}_\beta}\right)^{1/2}\approx0.29\frac{M\hbar\omega_\beta}{\mathcal{E}_\beta/\Delta\beta}.\tag{12}$$

[In the final expression, M is in nuclear mass units, $\mathcal{E}_b$ and $\hbar\omega_\beta$ are in MeV.] Even for $M=238/2$, $\mathcal{E}_b/\Delta\beta\approx5.8$ MeV, and $\hbar\omega_\beta=1$ MeV, this number is only about unity—not large compared with unity. Hence dynamics must be considered.

It is of interest to contrast the present situation with usual Coulomb excitation.[4,5] In the latter case, the excitation cross section generally decreases with ξ. This

[4] L. C. Biedenharn and P. J. Brussaard, *Coulomb Excitation* (Oxford University Press, New York, 1965).

[5] In an unpublished report L. C. Biedenharn and R. M. Thaler have specifically considered Coulomb excitation leading to fission.

can be understood by observing that during the collision, the nucleus is lifted into an excited state and then lowered back down to the ground state. If ξ is large, there is a high probability of returning to the ground state. In the present case, the nucleus is lifted through many states of collective excitation. If it reaches the barrier state, fission occurs. If it does not reach the barrier, it is gently lowered back to the ground state, as is demonstrated in Sec. IV D.

IV. DYNAMICAL CALCULATIONS

A. Thresholds

In the following calculations, we assume a cubic form for $\mathcal{E}(\beta)$:

$$\mathcal{E}(\beta)=3\mathcal{E}_b\left(\frac{\beta-\beta_0}{\Delta\beta}\right)^2\left[1-\frac{2}{3}\left(\frac{\beta-\beta_0}{\Delta\beta}\right)\right], \qquad (13)$$

but the expression is not used for β appreciably larger than β_b. We will also take B equal to a constant. Then the equations of motion corresponding to the energy expression (5) with zero impact parameter and $\theta=\theta'=\pi/2$ is

$$B\frac{d^2\beta}{dt^2}=-\frac{\partial\mathcal{E}}{\partial\beta}+\left(\frac{9}{80\pi}\right)^{1/2}\frac{zZe^2R_0^2}{r^3(t)}, \qquad (14)$$

where $r(t)$ satisfies the equation

$$M\ddot{r}=zZe^2/r^2. \qquad (15)$$

The equations can be cast into dimensionless form by introducing the variables

$$\begin{aligned} x&=(\beta-\beta_0)/\Delta\beta,\\ \rho&=r/r_c=Er/zZe^2,\\ \tau&=t(2E/Mr_c^2)^{1/2}, \end{aligned} \qquad (16)$$

and we note that $\omega_\beta^2=6\mathcal{E}_b/B(\Delta\beta)^2$. Then we obtain

$$\frac{1}{\xi_0^2}\frac{d^2x}{d\tau^2}=-\left(\frac{E_{\text{th}}^\infty}{E}\right)^3x(1-x)+\tfrac{1}{4}\rho^{-3}(\tau), \qquad (17)$$

with $\rho(\tau)$ the solution of the dimensionless Coulomb problem

$$\frac{d^2\rho}{d\tau^2}=\frac{1}{2\rho^2};\quad \rho(0)=1;\quad \rho'(0)=0. \qquad (18)$$

E_{th}^∞ is given by Eq. (9) and ξ_0 by Eq. (12). In numerical calculations, it was convenient to introduce $d\rho/d\tau=u$ as the independent variable instead of τ:

$$\begin{aligned} &\rho(u)=(1-u^2)^{-1},\\ &\frac{d}{d\tau}=\frac{1}{2\rho^2}\frac{d}{du};\quad \frac{d^2}{d\tau^2}=\frac{1}{4\rho^4}\frac{d^2}{du^2}-\frac{u}{\rho^3}\frac{d}{du},\quad -1\le u\le 1. \end{aligned} \qquad (19)$$

The collective adiabaticity parameter ξ_0 enters naturally into Eq. (17). When $\xi_0=\infty$, the right-hand side of (17) must also equal zero (if it can). The maximum value of ρ^{-3} is unity; at the inflection point, $4x(x-1)$ is also unity. This verifies the interpretation of E_{th}^∞.

Numerical results derived from Eq. (17) are presented in Fig. 2. $E_{\text{th}}/E_{\text{th}}^\infty$ is presented as a function of ξ_0. Also exhibited are the maximum kinetic energy and the radius of closest approach for assumed values of $\mathcal{E}_b$ and $\Delta\beta$. The maximum kinetic energy is of importance to the question of adiabaticity, as is discussed in Sec. V A.

We will find in the next section that there exist some cases where perpendicular orientation of the target is not the most favorable to fission, so that the fission threshold is lower than that calculated from Eq. (17). This occurs for small $\Delta\beta$, and may be a reflection of the simplified model, particularly the restriction to axial shapes ($\gamma=0$).

B. Cross Sections

The differential cross section corresponding to the backward scattering of the projectile has been calculated. This involves performing calculations for various initial orientations of the target, and determining which orientations lead to fission. Then the center-of-mass cross section is

$$\frac{d\sigma}{d\Omega}(180°)=\left(\frac{r_c}{4}\right)^2P, \qquad (20)$$

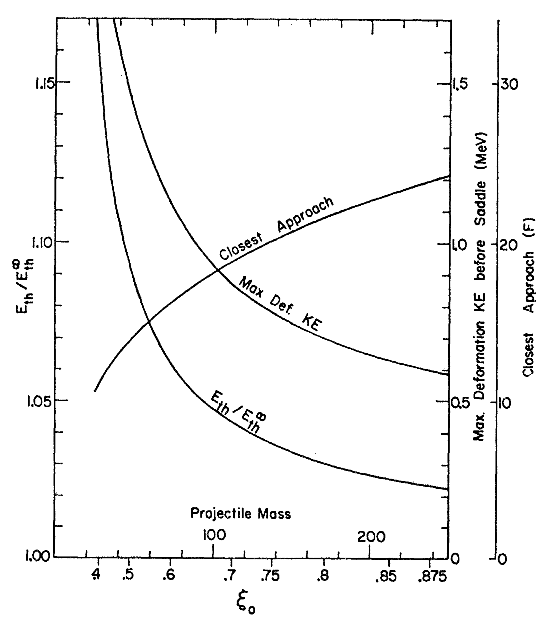

FIG. 2. Threshold calculations based on Eq. (17). $E_{\text{th}}/E_{\text{th}}^\infty$ is given as a function of the collective adiabaticity parameter ξ_0. The corresponding projectile mass (with appropriate charge) is also plotted along the abscissa for a U^{238} target. The maximum deformation kinetic energy and the closest approach are given for such a target with $\Delta\beta=1.0$. For other targets we note that KE $\propto \mathcal{E}_b/\Delta\beta$ and $r_c\propto(\Delta\beta/\mathcal{E}_b)^{1/3}$.

where $(r_c/4)^2$ is the Coulomb differential cross section, and P is the fraction of orientations leading to fission.

The equations of motion corresponding to the energy expression (5) are (still zero impact parameter)

$$\frac{d}{dt}(B\dot{\beta}) = -\frac{\partial \mathcal{E}}{\partial \beta} + \left(\frac{9}{80\pi}\right)^{1/2} \frac{zZe^2R_0^2}{r^3} P_2(\cos\theta) + \frac{1}{2}\frac{\partial \mathcal{I}}{\partial \beta}\dot{\theta}^2 + \frac{1}{2}\frac{\partial B}{\partial \beta}\dot{\beta}^2, \qquad (21)$$

$$\frac{d}{dt}(\mathcal{I}\dot{\theta}) = \left(\frac{9}{80\pi}\right)^{1/2} \frac{zZe^2R_0^2\beta}{r^3} 3\cos\theta\sin\theta.$$

In calculations reported here, the target was assumed to have the characteristics displayed in Table I. The cubic form was assumed for $\mathcal{E}(\beta)$, and B was taken to be a constant. Two functional forms were tried for $\mathcal{I}(\beta)$. These were $\mathcal{I} \propto \beta$ and $\mathcal{I} \propto \beta^2$. In both cases, the proportionality constant was chosen to fit the observed $\mathcal{I}(\beta_0)$.

The results are presented in Figs. 3–5. Note the insensitivity to the functional form of $\mathcal{I}(\beta)$. The differential cross sections are strikingly large, achieving values the order of hundreds of millibarns (because P can become close to unity). A "picture" of the collision process is presented in Fig. 6.

TABLE I. ${}_{92}U^{238} \rightarrow {}_{38}Sr^{97} + {}_{54}Xe^{141}$.[a]

Parameter	Value	Refer to
β_0	0.25	Fig. 1
$\mathcal{E}_b$	5.8 MeV	Fig. 1
$\hbar\omega_\beta = \hbar\omega_b$	1 MeV	Fig. 1
s_0	9.2 F	Eq. (4)
T	181.2 MeV	Eq. (22)
μ	$57.5m_p$	Eq. (23)
$(\Delta\beta)^2B(0)$	$1444.2m_p$ F^2	Fig. 8, Eq. (24)
$\mathcal{I}(\beta_0)$	$2500m_p$ F^2	Fig. 9, Eq. (25)
$3\hbar^2/\mathcal{I}(\beta_0)$	50 keV	...
g_2	1.34	Eq. (26)
g_3	0.517	Eq. (26)

Variable parameters of Eq. (22)

	$\Delta\beta = 0.5$	$\Delta\beta = 1.0$	$\Delta\beta = 1.5$
n	2	3	3
g_1	1.08×10^4 MeV/F^2	1.10×10^5 MeV/F^3	6.30×10^4 MeV/F^3

[a] The basic data assumed in compiling this table correspond roughly to the experimental data available, as given by Ref. 1.

C. Angular Distributions of Fragments

When calculating thresholds and cross sections, it was only necessary to carry on the progress of the target to the saddle point. For the calculation of fragment angular distribution, it is necessary to follow the target to the point of scission or beyond. Once the fragments are well separated, their trajectories can be continued by assuming that they behave like point particles interacting through a pure Coulomb field. It is necessary, therefore, to specify $\mathcal{E}(\beta)$, $B(\beta)$ and $\mathcal{I}(\beta)$ over a large range of arguments. These functions were parametrized as follows:

(1) $\mathcal{E}(\beta)$ was chosen here to be a cubic for $\beta \lesssim \beta_b$. At large separation of the fragments, $\mathcal{E}(\beta) = Z_1Z_2e^2/s - T$, where s is defined in Eq. (4) and T is the energy release

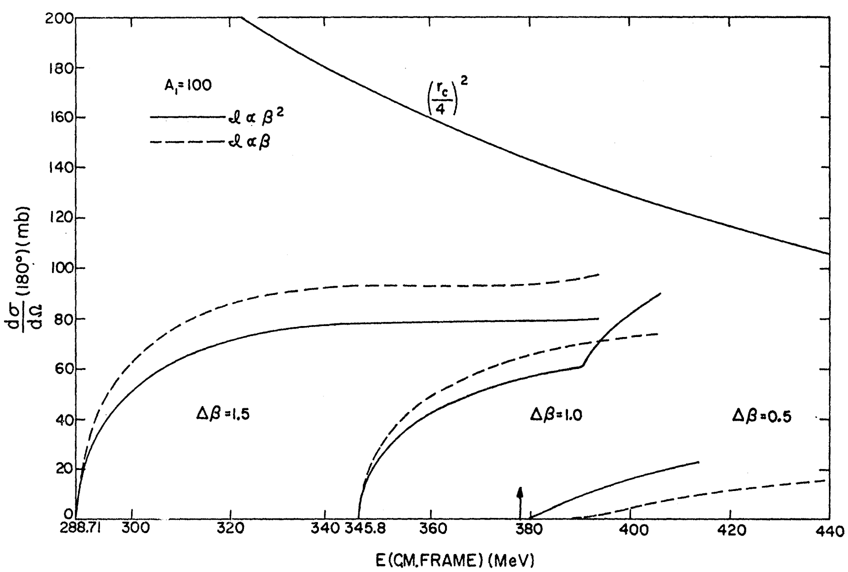

FIG. 3. Differential cross section in the center-of-mass system for fission, for $A_1 = 100$. $(r_c/4)^2$ is the elastic Coulomb cross section at 180°, and is the maximum possible. The arrow indicates the point where the closest approach equals to the range of nuclear forces, assuming $r_0 = 1.4$ F. This is more restrictive than the estimate of 1.2 F used in Eq. (10). Fission normally first appears for the target oriented perpendicular to the projectile direction. As the energy increases, the fission region fills an expanding angular region bounded by two cones. In some cases, a "second threshold" occurs when a new conic section opens up at small angles. This is reflected, for example, in the $\Delta\beta = 1.0$ curves. In some cases, the calculations for $\Delta\beta = 0.5$ actually exhibit a threshold at 0° before the 90° cone opens. Because of solid-angle considerations, this is a less sharp threshold, as can be noted by the flatness of some of the $\Delta\beta = 0.5$ curves.

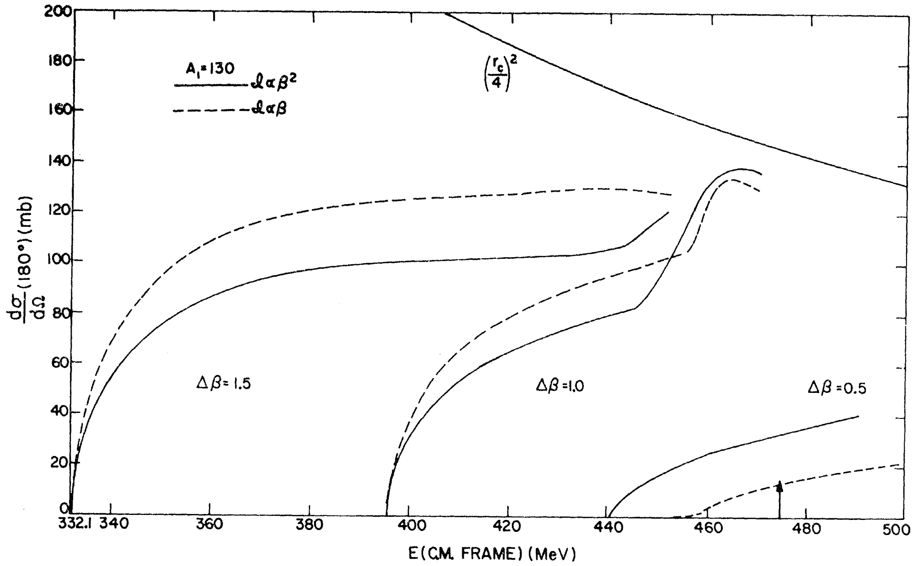

FIG. 4. Differential cross section in the center-of-mass system for fission, for $A_1=130$. See caption to Fig. 3.

of the reaction. [We take $\mathcal{E}(\beta_0)=0$.] In order to join the cubic to the pure Coulomb form, a term of the type s^{-n} was also included. This was to provide smooth interpolation between the two forms. The coefficient of this last term was chosen so that a smooth join could be made at some point $\beta_1>\beta_b$. In summary

$$\mathcal{E}(\beta)=3\mathcal{E}_b\left(\frac{\beta-\beta_0}{\Delta\beta}\right)^2\left[1-\frac{2}{3}\left(\frac{\beta-\beta_0}{\Delta\beta}\right)\right],\quad \beta<\beta_1$$

$$=\frac{Z_1Z_2e^2}{s}-\frac{g_1}{s^n}-T,\quad \beta>\beta_1. \tag{22}$$

$\mathcal{E}(\beta)$ is exhibited in Fig. 7.

(2) $B(0)$ was determined such that $\omega_\beta=[C_\beta/B(0)]^{1/2}$ yielded the observed β-vibrational frequency, with $C_\beta=6\mathcal{E}_b/(\Delta\beta)^2$ (see previous section). For well-separated fragments, we used the condition

$$\tfrac{1}{2}B\dot{\beta}^2=\tfrac{1}{2}\mu\dot{s}^2=\frac{1}{2}\left(\frac{\mu s_0^2}{4\beta}\right)\dot{\beta}^2, \tag{23}$$

where $\mu=m_1m_2/(m_1+m_2)$. An interpolation formula was used to join the $B=B(0)$ and the $B\propto\beta^{-1}$ limiting forms [see Fig. 8]:

$$B(\beta)=\frac{B(0)}{[1+(\beta/\beta_2)^2]^{1/2}}, \tag{24}$$

where β_2 is the point where $\mu s_0^2/4\beta_2=B(0)$. Note that $B(\beta_b)<B(\beta_0)$, so that $\omega_b>\omega_\beta$.

(3) $\mathcal{J}(\beta_0)$ is tied down experimentally (see previous section). The limiting form of $\mathcal{J}(\beta)$ for well separated fragments is

$$\mathcal{J}(\beta)=\mu s^2=\mu s_0^2\beta. \tag{25}$$

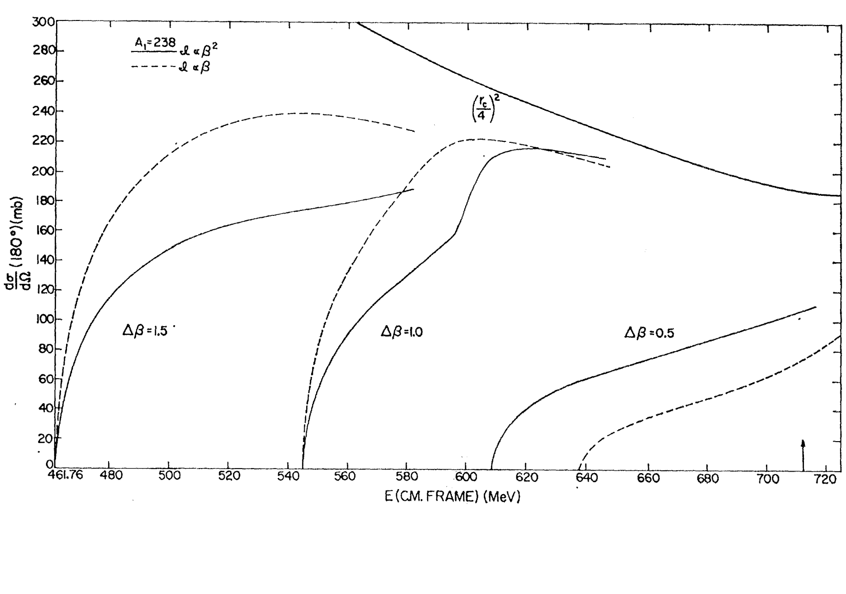

FIG. 5. Differential cross section in the center-of-mass system for fission, for $A_1=238$. See caption to Fig. 3.

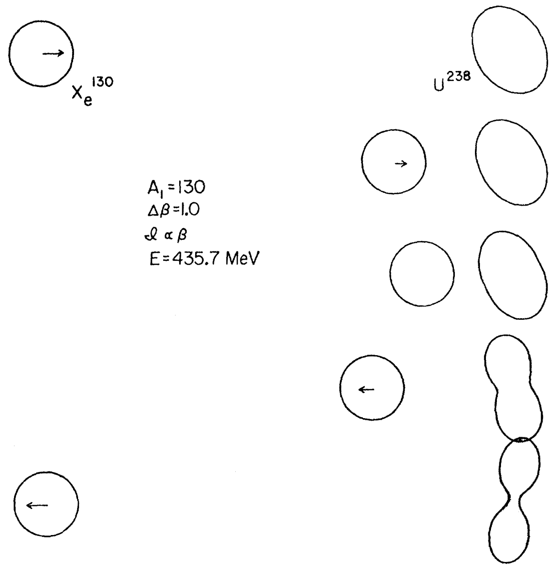

FIG. 6. Pictorial representation of a calculated encounter. The process can be seen to be quite analogous to tidal action, except for the repulsive nature of Coulomb forces.

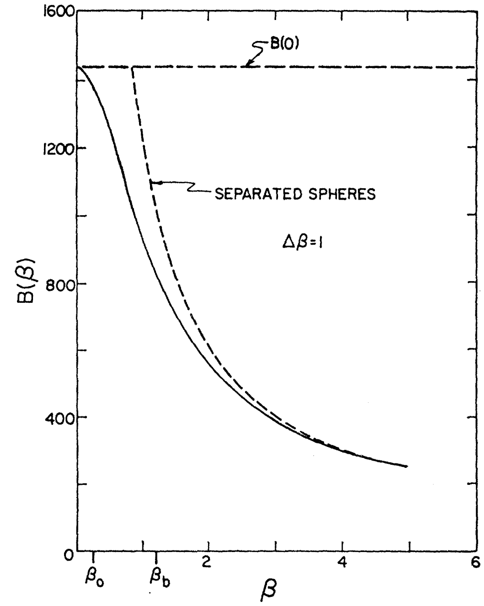

FIG. 8. $B(\beta)$ as given by Eq. (24). Note that $B(\beta_0)<B(0)$.

Again, interpolation was invoked [see Fig. 9]:

$$\mathcal{I}(\beta)=\mu s_0^2\beta((\beta+g_2)/(\beta+g_3)), \tag{26}$$

where g_2 and g_3 are constants, one combination of which was adjusted to fit the observed $\mathcal{I}(\beta_0)$ and the other was rather arbitrarily chosen.

The parameters employed, in addition to those tabulated in the previous section, are listed in Table I.

The immediate result of integrating Eqs. (21), and analytically continuing to infinite separation, is the final fragment pair angle θ_f (in their own center-of-mass system) as a function of the initial target orientation θ_i. Since all initial orientations are equally probable (equal probability in $\cos\theta_i$), the probability of fissioning into

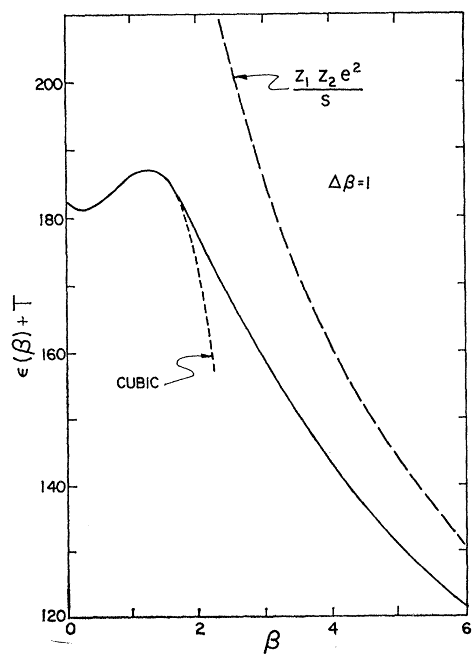

FIG. 7. $\mathcal{E}(\beta)$ as given by Eq. (22). The short-dashed curve is the cubic approximation. The long-dashed curve is the pure Coulomb interaction.

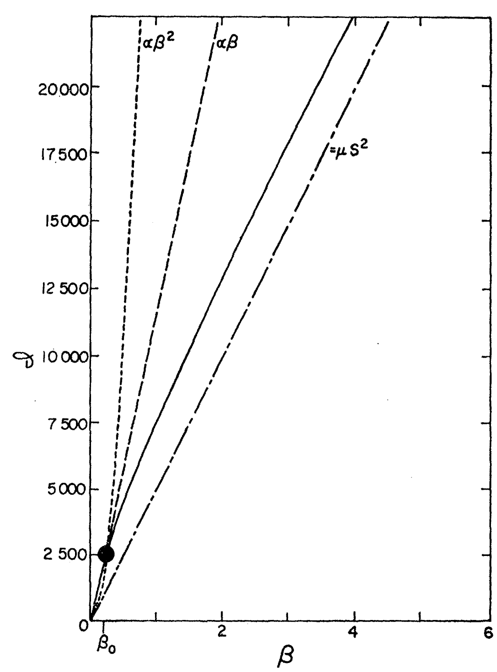

FIG. 9. $\mathcal{I}(\beta)$ as given by Eq. (26). The various broken curves give other approximations. The black circle is the experimental value determined from the rotational spectrum of U^{238}.

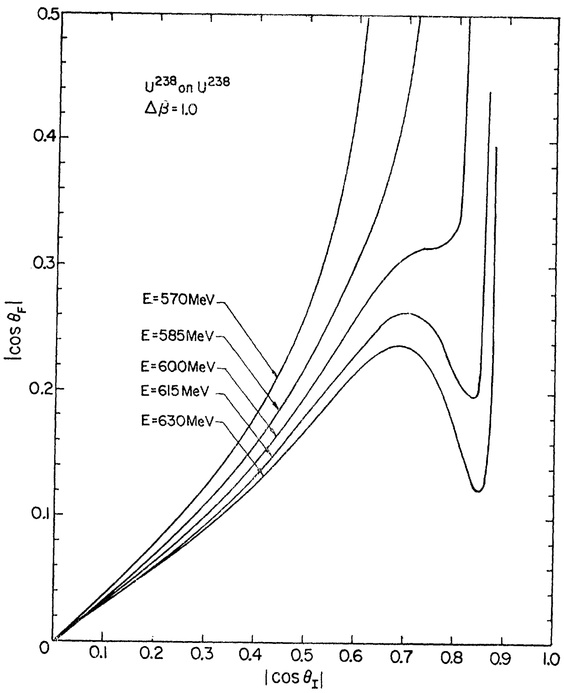

FIG. 10. Final fragment orientation as a function of initial orientation for a particular example. If the curves were carried further, these would end in a converging zigzag (see text).

$d|\cos\theta_f|$ is

$$\frac{dP}{|d\cos\theta_f|}=\frac{|d\cos\theta_i|}{|d\cos\theta_f|}. \tag{27}$$

Curves of $|\cos\theta_f|$ as a function of $|\cos\theta_i|$ are shown in Fig. 10. As the initial angle of the target approaches a value where fission will no longer occur, the final angle increases rapidly. Indeed, there is a critical initial angle for which the nucleus ends up sitting at some deformation $\beta_b > \beta > \beta_0$, and rotating. Therefore, the curves in Fig. 10, which all end up increasing, should actually exhibit rapid zigzags (because the ordinate is $|\cos\theta_f|$) which cease at the "threshold" angle. Our calculations did not attempt to sweep out such fine detail.

The angular distributions of the fragments are shown in Fig. 11. Spikes occur whenever the corresponding $|\cos\theta_f|$ versus $|\cos\theta_i|$ curve has a zero derivative. The spikes are very narrow and are, of course, integrable.

The fragment angular distributions are generally concentrated around the direction at right angles to the beam. The width of the distribution increases with decreasing $\Delta\beta$. Since the distributions are so very narrow, the threshold behavior would appear to be a better experimental measure of $\Delta\beta$ than the angular distribution. The angular distributions can be an effective tag in identifying the process, however.

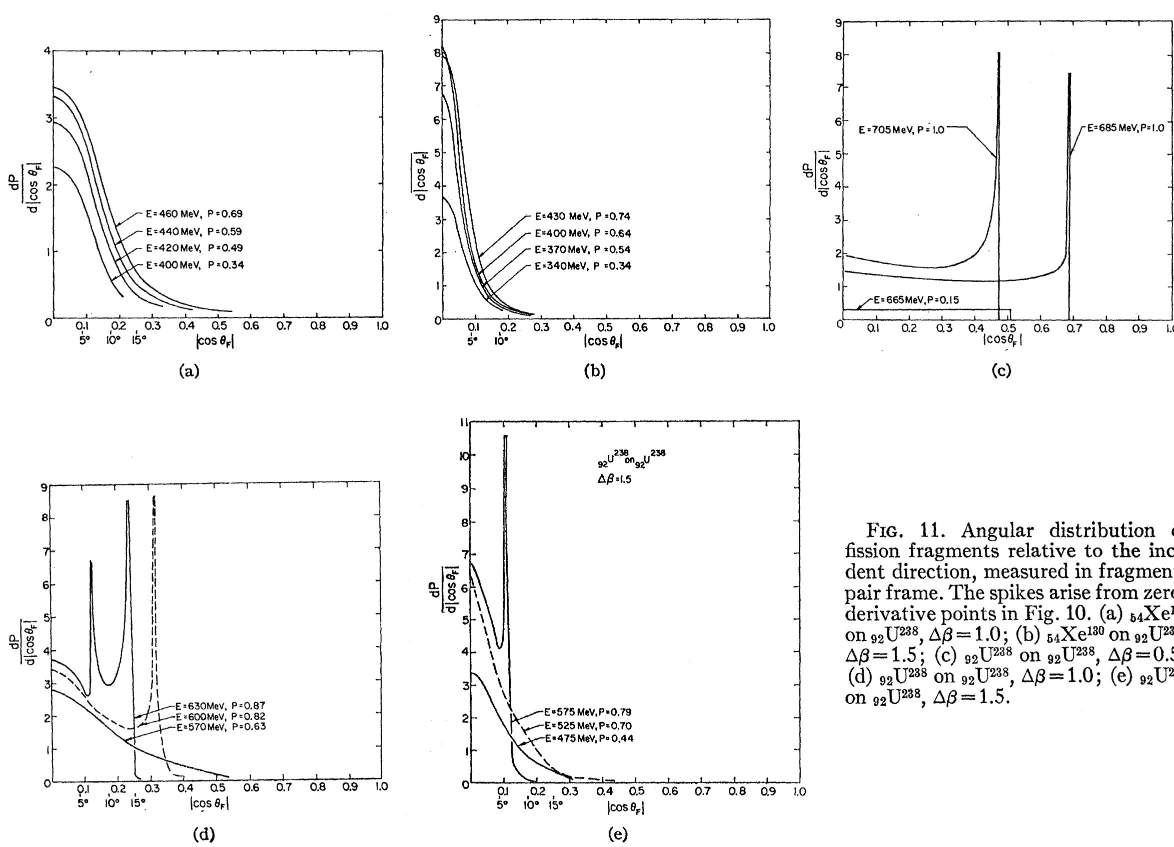

FIG. 11. Angular distribution of fission fragments relative to the incident direction, measured in fragment-pair frame. The spikes arise from zero-derivative points in Fig. 10. (a) $_{54}Xe^{130}$ on $_{92}U^{238}$, $\Delta\beta=1.0$; (b) $_{54}Xe^{130}$ on $_{92}U^{238}$, $\Delta\beta=1.5$; (c) $_{92}U^{238}$ on $_{92}U^{238}$, $\Delta\beta=0.5$; (d) $_{92}U^{238}$ on $_{92}U^{238}$, $\Delta\beta=1.0$; (e) $_{92}U^{238}$ on $_{92}U^{238}$, $\Delta\beta=1.5$.

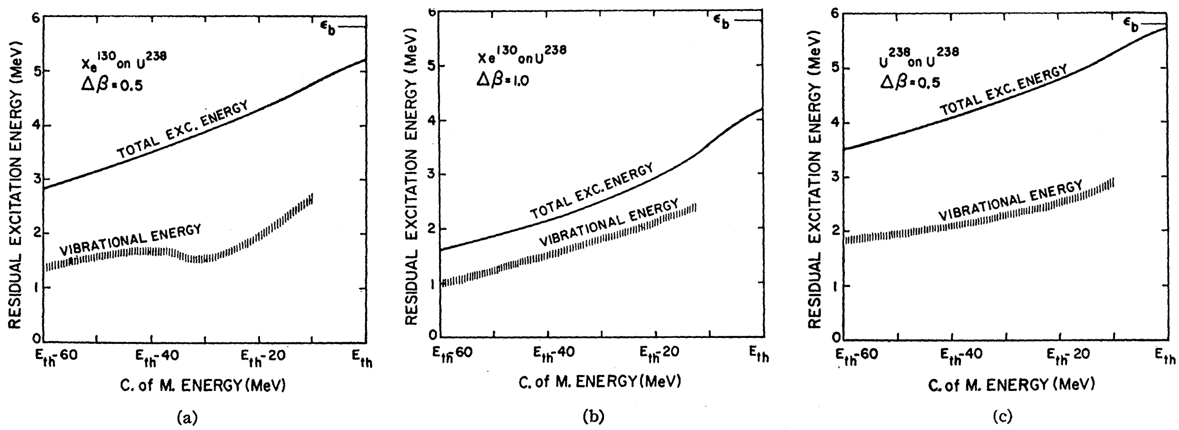

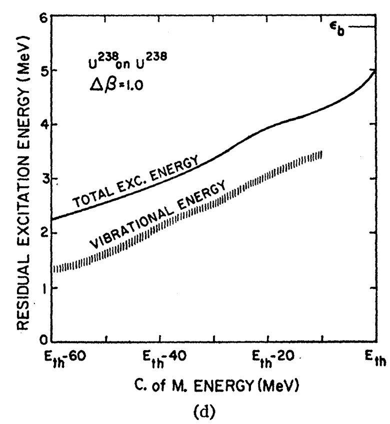

FIG. 12. Residual excitation energy produced by Coulomb excitation below the fission threshold. The breakdown of total excitation energy into rotational and vibrational parts is not unique in the calculation because of coupling between the modes.

D. Collective Excitation below Fission Threshold

At energies below the fission threshold, the collision can leave the target in an excited collective state. For slow collisions, the probability is small, but as the fission threshold is approached, the energy deposited into the target approaches $\mathcal{E}_b$. For a target properly oriented, the collective energy is just equal to $\mathcal{E}_b$ at threshold, but since we must average over initial orientations, the mean energy is always less than $\mathcal{E}_b$.

Since our calculations are classical, we can calculate only the mean energy of excitation, not the probability of exciting particular quantum states. The results are displayed in Fig. 12. When the residual collective excitation energy is large, it is not meaningful to separate rotational and vibrational energies, although such a separation can be made approximately at low excitation. That is why the vibrational curves are not extended up to E_{th}.

V. FURTHER REMARKS

A. Intrinsic Adiabaticity

An essential feature in the interpretation of Coulomb fission is that the nucleus remain on the lowest-energy surface, i.e., that there be no intrinsic excitation. The adiabatic condition in this sense is distinct from the question of whether the collision is "slow" as discussed in Sec. III.

Collective motion as a mechanism of exciting intrinsic states has been considered in the literature.[6] It is evident that an appreciable energy gap above the ground state is effective in inhibiting intrinsic excitation. For even-even nuclei, such a gap indeed exists, and is expected to increase with deformation. Kennedy, Wilets, and Henley[7] give the expression

$$2\Delta \approx 25.6A^{-1/2}[1+(3/4\pi)\beta^2] \text{ MeV}, \qquad (28)$$

or about 1.6 MeV. In a semiclassical treatment of excitation (conserving energy), the gap cannot be jumped unless there is sufficient collective kinetic energy available. Even when a transition is energetically permitted, the existence of a gap is expected to inhibit excitation because of the coherent nature of the ground state.

B. Theories of the Energy Surface

There are three types of calculations currently capable of making predictions about the energy surface. Of

[6] L. Wilets, Phys. Rev. **115**, 372 (1959); *Theories of Nuclear Fission* (Oxford University Press, New York, 1964), p. 94.

[7] R. Kennedy, L. Wilets, and E. M. Henley, Phys. Rev. Letters **12**, 36 (1964).

these, the first has been available for 20 years, the second is now being exploited, and the third will probably make a quantitative appearance in a few years.

Detailed studies based on the Bohr-Wheeler[8] liquid-drop model began with Frankel and Metropolis[9] in 1947 and have reached a climax in a series of publications by Swiatecki and collaborators.[10] These calculations indicate a broad fission barrier with $\beta_b \sim 1.6$. [Because our β is defined to be proportional to the quadrupole moment according to Eq. (2), it is generally larger than the usual α_{20} expansion coefficient.] The liquid-drop model, of course, gives $\beta_0=0$. If we assume it gives β_b properly, and that β_0 is 0.25, then this would predict $\Delta\beta \approx 1.35$.

Independent-particle-model (IPM) states in a deformed potential have been calculated by Nilsson and others and the results have been successfully applied to the evaluation of a variety of nuclear properties. The energy levels have been summed by Mottelson and Nilsson[11] to determine the equilibrium deformation of deformed nuclei. Although there are fundamental uncertainties associated with this procedure,[12] they did obtain quantitative success. More recently Primack[13] and Gustafson *et al.*[14] have applied the approach to evaluating the energy surface out to the fission barrier. The results must be regarded as qualitative, but they do imply a considerably smaller $\Delta\beta$ (a few tenths) than the liquid-drop model.

As a matter of principle, it is not possible to determine the total energy of a nucleus as a function of deformation from the IPM levels alone (some further assumptions about the two-body force are required). Hartree-Fock calculations based upon effective two-body interactions face this issue, at least, even though they have their own uncertainties in the appropriate effective potentials. Several Hartree-Fock projects are now in operation, and it seems to be only a matter of time until they expand to the fissionable nuclei.

[8] N. Bohr and J. A. Wheeler, Phys. Rev. **56**, 426 (1939).
[9] S. Frankel and N. Metropolis, Phys. Rev. **72**, 914 (1947).
[10] S. Cohen and W. J. Swiatecki, Ann. Phys. (N. Y.) **22**, 406 (1963).
[11] B. R. Mottleson and S. G. Nilsson, Kgl. Danske Videnskab. Selskab, Mat. Fys. Skrifter **1**, No. 8 (1959).
[12] L. Wilets, Brookhaven National Laboratory Report No. BNL 948(C-46), 1965, p. 929 (unpublished).
[13] J. R. Primack, Phys. Rev. Letters **17**, 539 (1966).
[14] C. Gustafson, I. L. Lamm, B. Nilsson, and S. G. Nilsson (unpublished); also V. M. Strutinsky, Kurchatov Institute of Atomic Energy Report No. 1108, 1965 (unpublished).

It is fairly evident that Coulomb fission could provide a severe test of nuclear models. If it turns out that $\Delta\beta$ is so small that Coulomb fission cannot be induced for even the most fissile targets, then this would yield a bound for the models.

C. Further Refinements

The present calculations contain simplifications which ought to be removed. A more complete calculation would include the following:

(1) The shape parameter γ should be treated as a dynamical variable.

(2) A more general potential surface should be allowed.

(3) The projectile trajectory $\mathbf{r}(t)$ should also be treated as a coupled, dynamical variable.

(4) Nonzero impact parameters should be considered. This immediately implies that the Euler angles φ and ψ must also be included.

Several of these generalizations are currently under investigation by Dr. C. Y. Wong. Probably the most significant aspect is the "unfreezing" of the γ motion.

VI. EXPERIMENTAL SUGGESTIONS

On the basis of our calculations, we propose experiments which incorporate the following features in order to establish and study the effect.

(1) Even-even fissile targets. The lower the fission barrier, the more likely it will be to observe the effect.

(2) The heaviest projectiles available at variable energies exceeding the estimate of Eq. (9).

(3) Coincidence of fission with the scattered projectile, particularly into the backward directions. For this purpose, the projectile must be at least somewhat lighter than the target. The use of coincidence is invaluable in experiments involving targets which undergo spontaneous fission.

(4) Observation of the fragment angular distribution.

(5) If fission is not observed under the most favorable conditions up to energies where nuclear interactions begin, then the de-excitation of the collective states should be studied.

ACKNOWLEDGMENT

We wish to thank Dr. C. Y. Wong for helpful discussions.